Journal of Data Acquisition and Processing
ISSN: 1004-9037
https://sjcjycl.cn/
DOI: 10.5281/zenodo.776699

HIGH DENSITY NOISE FILTER METHOD FOR DENOISING MAMMOGRAM BREAST CANCER IMAGES

Suriya Priyadharsini .M[1], Dr. J. G. R. Sathiaseelan[2]
[1]Research scholar, Department of Computer Science, Bishop Heber College (Affiliated to Bharathidasan University), Trichy, Tamilnadu, India
julimca.sigc@gmail.com
[2]Associate Professor, Department of computer Science, Bishop Heber College (Affiliated to Bharathidasan University), Trichy, Tamilnadu, India
jgrsathiaseelan@gmail.com

Abstract

Mammography analysis is a crucial tool when it comes to detecting breast cancer early. While analyzing a mammogram, the most crucial stage is the pre-processing because of the low quality of the original picture recorded. In order to fix and alter the mammography picture, pre-processing is crucial. A wide variety of pre-processing methods are at your disposal. Images taken from a Mammogram may include noise due to fluctuations in lighting and sensor inaccuracy. If these sounds can be eliminated without compromising the image's borders and small characteristics, a proper diagnosis of breast cancer may be made using imaging technology. In this study, we present a High-Density Noise Filtering (HDNF) technique for denoising digital mammography pictures. Experiments on a dataset including a wide range of mammography pictures test the effectiveness of the proposed technique against a variety of image quality measures. When the pictures have been denoised, a Region of Interest (ROI) technique based on statistical moments is proposed for locating suspicious areas in breast cancer images of varying modalities. When a ROI has been identified, its borders in the resulting subtracted picture must be defined. A Canny edge detection technique is used for this purpose. Mean square error, peak signal-to-noise ratio, and the Structural Similarity Index Method (SSIM) are used to evaluate the effectiveness of the Wiener Filter (WF), Gaussian Filter (GF), the Adaptive Median Filter (AMF), and the Hidden Markov Model (HDNF). Results from the experiment are presented in the form of a quality-of-images-measures comparison between the original, unscathed pictures and denoised versions of the same images affected by varied levels of generated salt-and-paper-noise and speckle-noise. The HDNF technique produces a higher quality result than the related filter strategy.

Keywords: Mammogram, Denoising, ROI, WF, GF, AMF, HDNF, Canny edge detection.

1. Introduction

Breast cancer has become one of the commonly occurring cancers in women, particularly in developing countries. It is a life-threatening disease and can be treatable if early detected. For women with or without signs of breast cancer, Mammogram has proven to be the most effective and consistent method for early diagnosis. [1, 2]. It is a screening and analytic technique for the human breast that uses low-energy X-rays to evaluates the breast. A digital mammography

technique called full-field digital mammography (FFDM) replaces previous x-ray sheets with an electronic area that converts x-ray films into digital mammographic images of the breast. As a result of this, mammogram images are of higher quality and needless radiation exposure. Physicians use computers to analyzed and interpret breast images. This allows for a more accurate diagnosis of breast abnormalities and increases the chances of survival [3]. Breast cancer may be detected earlier with mammography than with any other screening approach. With the introduction of mammography screening programs, the number of women losing their lives to breast cancer has decreased by 30-70%. Benign tumors are those that are not malignant, whereas malignant tumors are the other kind. Growth is normal, but metastasis is unusual in benign tumors. Even in other organs, a malignant tumor might continue to develop and disseminate. Contrast Enhancement, Grayscale conversion, Image Resizing and image denoising plays an significant role in improving the quality of digital images and medical diagnosis as a pre-processing step in medical imaging systems and applications. Medical image denoising has been studied for a long time in a variety of fields, but it remains a difficult problem to solve. It's because, from a mathematical perspective, medical image denoising is a reversible issue with no unique and flexible solution. When the images have been denoised, a Region of Interest (ROI) technique based on statistical moments is proposed for locating suspicious areas in breast cancer images of varying modalities. After removing the clutter, the image must be refined by identifying the items' edges. An edge detection method is used for this purpose.

2. Related work

Duo-Median, suggested by **Vikramathithan [2020],** has been used to assess the software's ability to remove salt-and-pepper noise. This median has a density of up to 95% in the Lena picture for general comparison, and in the Mammogram image used for medical image pre-processing. There are superior results with Duo-Median filter for PSNR and SSIM than with Lena image noise density above 80% and in mammograms above 90% noise density. The demonstration is performed with quantitative results and visual images when it comes to de-noising, the proposed Dual-Median Filter is on par with SUMF in terms of effectiveness.

Shakil Mahmud Boby's [2021] research assesses the effectiveness of 8 several methods of denoising filtering based on RMSE, PSNR, MAE, and SSIM for four of the most damaging types of noise, such as speckles and salt and pepper, Poisson, and Gaussian. All of these sounds and filtering procedures are used to the three medical images that are used the most often, which are ultrasound (US), CT, and MRI. Both statistical and visual-qualitative approaches are used in the analysis of performances. The Gaussian filter is the most effective method for despeckling images obtained from MRI, CT, and US. The median filtering method performs far better than any other US, CT, or MRI imaging when it comes to salt and pepper noise. When trying to reduce Poisson noise from medical imaging, the anisotropic diffusion filtering strategy is the one that is recommended (US, CT, MRI). In conclusion, it would seem that the non-local means filtering technique is the most effective one for getting rid of the Gaussian noise in the MRI, CT, and US pictures. It is also essential to point out that they carried out the same study with respect to other medical imaging modalities, such as X-ray, PET (Positron Emission

Tomography), and OCT (Optical Coherence Tomography). Most significantly, the sorts of findings that are obtained in each instance are similar to one another.

Suneetha Mopidevi [2020] proposed approach is associated with reduced complexity, which stems from the fact that the system design and optimization time are both time-consuming. The results reveal that they are efficient at remove noise from medical ultrasonography and MRI images. The results of the proposed method are remarkable in that noise is reduced while the structure remains intact. Nonetheless, it is depicted that the suggested strategy performs better than existing techniques in terms of image fidelity, image quality index, peak SNR, and PSNR.

As **Siyi Tang [2021]** discovered, removing data from training with high Shapley values reduces the performance of the model for detecting pneumonia, whereas removing data with low Shapley values improves the quality of the model. There were more misidentified cases and much more instances of pneumonia in low-value data and high-value data, respectively, as measured by the Shapley values. Yet, a low Shapley value may signify mislabeled or low-quality photos, while a high value suggests data that is suitable for pneumonia diagnosis. The method may be utilized as a template for denoising large medical imaging datasets.

Using the CNN approach, **Pallavi Bora [2021]** evaluates the most extensively used image denoising algorithms, concluding that the greatest performance and increasing PSNR value for the bilateral filter should be found based on the data. To improve the image denoising approach, they need to find a higher PSNR value.

Rashid Mehmood Gonda [2020] proposed a Hybrid denoising method for mammogram images. There are two steps to the hybrid technology that has been proposed: First, mathematical morphology was used as a pre-processing technique for image enhancement. After de-noising, a global unsymmetrical trimmed median filter (GUTM) is applied to it. For mammogram images, experimental findings depict that the suggested technique performs effectively. An alternate denoising strategy was found in this study.

3. Pre-processing

An effective image preprocessing technique is required to eliminate noise from mammogram images and to improve image quality before further processing and analysis. This process removes the background from the mammogram, making it easier to search for abnormalities and decreasing the computational complexity involved. Medical pictures, like digital mammograms, are notoriously difficult to analyze and interpret, yet accuracy is of the utmost importance in the results. For better image quality and more accurate segmentation findings, a pre-processing stage must be carried out. It is more difficult to remove noise from a mammogram image. Patients' ailments could only be diagnosed by doctors using clear images. To reduce noise from mammograms from the past two decades, a lot of research was done. To denoise, an image, a variety of filtering approaches were presented. To remove noise from mammogram images, four distinct filtering algorithms with the proposed algorithm are used in this work. The MSE, PSNR, and SSIM values can be compared to get the best filter.

3.1 Gray Scaling

The procedure for converting an image to greyscale from various color spaces, such as RGB, CMYK, HSV, and so on, is referred to as gray scaling. It might be completely dark or completely light at various points.

3.1.1 Importance of Gray scaling

- **Dimension reduction:** For instance, a grayscale image only has one dimension, but an RGB image contains three color channels and hence three dimensions.
- **Reduces model complexity:** We might use RGB photos that are 10x10x3 pixels in size for training the neural article. The number of input nodes in the input layer will be set at 300. Grayscale pictures, on the other hand, only need 100 input nodes for the same neural network.

3.2 Image Resizing

Image scaling is an essential part of the image processing approach, as it allows one to increase or decrease the provided picture size while maintaining its pixel format. The process of image interpolation may be broken down into two distinct sub-processes: image down-sampling and image up-sampling. Both of these sub-processes are required when scaling the data to meet either the particular communication channel or the output display. Even if it is more time and energy economical to send the client versions with a lower resolution, it is possible that some approximation of the original high resolution would be required in order to provide the final visual data. In a wide variety of applications, including but not inadequate to various consumer items as well as key tasks within the medical, security, and military industries, an accurate resizing of picture data is a crucial step that must be taken.

4. Types of Noises Affected on Mammogram Images

Noise refers to the unintentional fluctuations or changes in clarity or color information that might occur during the picture capturing process. It's a method that reduces the quality of a photo by adding something to it that wasn't there to begin with. Salt and pepper noise, poisson noise, and gaussian noise are the most common type of noise that appear in mammograms. Inaccurate diagnoses may be made due to these disruptions, which prevent precise analysis and inaccurate interpreting of the breast picture recorded during a mammographic test. Imperfect mammograms may be traced back to faulty steps in the image collecting process, which will have repercussions across the whole image processing and diagnostic procedures.

4.1 Salt and Pepper Noise

When a spike noise model is applied to a picture, dark pixels would replace bright ones, and brilliant ones would appear as black and white dots (also known as impulsive noise or fat-tail distributed noise). Subtle alterations to the image are introduced by the "salt and pepper" noises caused by the acute and sudden changes in the video stream.

4.2 Gaussian Noise

It is based on Gaussian distribution and is additive when it comes to this model of noise. In other words, this noise has the same probability density function as a normal distribution or Gaussian distribution. Gaussian noise has a specific instance called white noise, in which the

values are statistically independent. It is computationally simpler to utilize additive white Gaussian noise in most situations.

4.3 Speckle Noise

Speckle noises are the most common cause of image quality reduction in radar images. Typically, conventional radar's granular noise is brought on by the object's return signal creating random oscillations. Speckle noise would increase the mean grey level of a particular region, making it more difficult to understand pictures in SAR data. Coherent processing of backscattered signals from several spatially separated objects is at the root of this phenomenon.

4.4 Poisson Noise

Poisson Noise, often known as shot noise, is a kind of random statistical fluctuation that may be seen in images. There are a lot of factors that cause noise in an image, such as a finite quantity of energy-carrying electrons in an electronic circuit or photons in an optical device.

5. Denoising Filters

5.1 Wiener Filter

The WF is a linear filter utilized to reduce noise in images by comparing the resulting picture to an idealized version of the signal without any disturbances. The image and noise are assumed to be linear stochastic processes with known spectrum characteristics, the filter is required to be causal and physically realizable, and its performance is measured in terms of the standard deviation of its mean squared errors (MMSE). Statistical approaches are the foundation of filtering. Inverse filtering is often used as a deconvolution restoration method. For a blurred picture to be recovered using inverse filtering, a high sensitivity to additive noise is required. Noise smoothing and inverse filtering are both guaranteed by the Wiener filter. Blurring is reversed, and additive noise is eliminated. The Wiener filter does a terrible job in the face of signal-dependent noise and destroys fine visual details while also blurring sharp edges.

5.2 Gaussian Filter

Gaussian filtering relies on the discovery of peaks. If peaks are impulses, this is the result. As an added bonus, this filter is useful since it modifies not only the targeted spectral coefficient but also any amplitude spectral coefficients that fall inside its frame. This filter is effective in reducing edge blur because it places more weight on pixels close to the edge. This filter is computationally efficient and features a smoothing level that may be adjusted by the user.

5.3 Adaptive Median Filter

There are two types of median filters: linear and nonlinear. While it does not alter the boundaries or reduce contrast, it is highly effective in removing impulse noise. However, it impacts all pixels, regardless of noise content, therefore it's a major problem. While the filtering process is ongoing, adaptive median filters change the window size to compensate for this. As in median filtering, it calculates the median value for each pixel and compares it to a threshold to determine whether to replace, keep, or increase the neighbourhood size and recalculate the pixel. As a result, it only affects the pixels in the image which have noise content. As a result, it is suitable for mammogram images.

5.4 Proposed algorithm

It is crucial to identify whether or not a pixel with a value of 0 (or 255) is noisy in order to successfully eliminate noise. If the uncorrupted pixel value in the window, for example, is less than 10 (or more than 245), then HDNF believes that all pixels with values of 0 (or 255) are noise-free pixels.

It's important to note that the threshold value of 10 is subject to alteration depending on the noise density of the images. Threshold value calculated using standard deviation. The optimistic square root of the variation is the standard deviation.

The Threshold standard deviation formula looks like this:

$$\sigma = \sqrt{\frac{\sum(X-\mu)^2}{N}} \quad (1)$$

X = each value

σ = Threshold standard deviation

∑ = sum of…

N = number of values in the pixel

μ = pixel mean

In Example 5.1,

$$\frac{(238 - 242.71428571429)2 + \ldots + (238 - 242.71428571429)2}{7}$$

$$= \frac{599.42857142857}{7}$$

$$= 85.632653061224$$

$$\sigma = \sqrt{85.632653061224}$$

$$= 9.2537912804009$$

So the Threshold value around 10.

The HDNF algorithm is as follows:

Let P: = [p(i; j)] Consisting of pixelsp(i; j), where i and j are in the range of 1 to n, respectively, is considered noisy.

Step 1. For all i and j,

Step 1.1 If p(i; j) is noisy, and at least one of the pixels in the window with a 3x3 size that accepts this as its center is noisy, then for all of the pixels i and j in the window if there is at least one p(i; j) such that or 245 < p(i; j) < 255 or 0 < p(i; j) < 10, then

- Find the maximum number of pixels in the window that are repeated;
- The median of the values should be calculated.

- Replace this value with p(i,j)

Step 1.2 If p(i; j) is noisy, and at least one of the pixels in the window with a 5x5 size that accepts this as its center is not noisy, then for all of the pixels I and j in the window if there is at least one p(i; j) such that or $245 < p(i; j) < 255$ or $0 < p(i; j) < 10$, then

- Find the maximum number of pixels in the window that are repeated;
- The median of the values should be calculated.
- Replace this value with p(i,j)

Step 1.3 If p(i; j) is noisy, and at least one of the pixels in the window with a (2k +1) x (2k + 1) size that accepts this as its center is not noisy, then for all of the pixels I and j in the window if there is at least one p(i; j) such that or $245 < p(i; j) < 255$ or $0 < p(i; j) < 10$, then

- Find the maximum number of pixels in the window that are repeated;
- The median of the values should be calculated.
- Replace this value with p(i,j)

Where $0 < k < \min [m,n]$

Step 2. Otherwise, keep the value of x(i; j).

Example 5.1: The I is a noisy image with a size of 512x512. For example, if I (40,41) is equal to 0, then the 3x3 window shown in Figure 1a is the window that accepts this pointer as the center pointer. This window has at least one non-noisy pixel; for example, p (39,41)≠ 0 (or p(39,41)≠ 255) then p(39,41) = 225. There is a pixel value among 245 and 255 in this window as well; for example, 245 < p (40,40) = 251<255. As a result, the criteria laid out in Step 1.1 can be considered met by this window. When this occurs, we find that 238 and 246 are the most frequently occurring values for individual pixels within the window, with 242 serving as the midpoint. So, we give the noisy pixel a value of 242, and with us window looks like in Figure 1.

238	225	246
251	0	255
0	246	238

238	225	246
251	242	255
0	246	238

Figure1. Noisy pixel windows

Example 2.2 supposes that P is a noisy image with a size of 512x512. Let used the 3x3 window indicated in Figure 2a to accept p (314,350) as the center pixel. This window's pixels are all

noisy. As a result, the window does not fulfill the criteria set out in Step 1.1. In Figure 2b, let the 5 × 5 sized windows accept the center pixel p (314,350). So at least one of the pixels in this window appears to be noise-free; for example, p (312,350)≠ 0 (or p (312,350)≠ 255), since p(312,350) = 6. There is a minimum of one pixel between 0 and 10 in this window. For example, 0 < p (314,348) = 6 < 10. The window satisfies the surroundings given in Step 1.2. As a result, the window's maximum repeating pixel values are discovered to be 0 and 6, and the median value is calculated as 3. Figure 2c displays the result of setting value 3 to the noisy pixel.

255	0	6	0	6
255	255	255	255	0
0	6	255	255	255
255	0	6	255	6
6	0	0	6	255

Figure2(a). 5x5 window

255	0	6	0	6
255	255	255	255	0
0	6	3	255	255
255	0	6	255	6
6	0	0	6	255

Figure2(b). 5 × 5 sized windows

255	255	255
6	255	255
0	6	255

Figure2(c). Setting value 3 to the noisy pixel.

6. Experiments and Discussion

The suggested approach is tested on a sample of breast mammograms obtained from the mini-Mammogram Image Analysis Society's database (MIAS). The suggested method's outcomes are going to be evaluated to those of other filters applied to the same photos. The computer language Python is used to actualize the suggested approach.

The deployment was executed on a laptop running Windows 10 and equipped with an Intel Core i7 Processor running at 2.2 GHz, along with 16 GB of Memory. In these investigations,

the assessment outcomes on the test pictures are evaluated based on the PSNR, MSE, and SSIM performance metrics.

- **Dataset Mammogram Images**

As can be seen in Figs. 3, 4, and 5, the dataset consists of eleven mammography images taken from the Mini-mammogram Imaging Analysis Society (MIAS) archive. The PGM format is used for every single picture in the test suite. These images are saved as JPGs and reduced in size to 256 by 256 pixels for the sake of the experiments.

- **Image Quality Evaluation Measures**

MSE and PSNR are two of the quantitative picture quality indicators used to evaluate the suggested image denoising algorithm. The original and the denoised images are used to calculate these metrics. The MSE is the sum of the squared differences between the original picture (O) and the denoised image (D) using a m and n matrix. If the approach works well and its MSE can be calculated, the value of the MSE would be low [10]:

$$\mathrm{MSE} = \frac{1}{\mathrm{M}*\mathrm{N}} \sum_{\mathrm{M,N}} [\mathrm{O}(\mathrm{m},\mathrm{n}) - \mathrm{D}(\mathrm{m},\mathrm{n})]^2 \quad (2)$$

The PSNR is the second measurement that may be used to provide a good indicator of the capabilities of the approach to eliminate sounds. The low value of PSNR for the denoised picture indicates that the quality of the image is subpar [10]. The PSNR may be determined using the equation that is provided here.

$$\mathrm{PSNR} - 10\log_{10}\left(\frac{\mathrm{R}^2}{\mathrm{MSE}}\right) \quad (3)$$

The highest pixel fluctuation in the preceding equation represents the image's dynamic range. If the image is a double floating-point, R is one, but if it's an 8-bit unsigned integer, it's 255.

- **Structure Similarity Index Method (SSIM)**

The Luminance Index, Contrast Index, and Structural or Correlation Term Index (SSIM) are the three primary factors used to determine a quality measuring metric in the SSIM index approach. This metric is the sum of the aforementioned three factors [11].

These three words define the Structural Similarity Index Method:

$$\mathrm{SSIM}(\mathrm{x},\mathrm{y}) = [\mathrm{l}(\mathrm{x},\mathrm{y})]^{\alpha}[\mathrm{c}(\mathrm{x},\mathrm{y})]^{\beta}[\mathrm{s}(\mathrm{x},\mathrm{y})]^{\gamma} \quad (4)$$

Here, l is luminance, which is used to compare the brightness of two images, c is contrast, which is used to distinguish the ranges between the brightest and darkest region of two images, s is structure, which is used to evaluate the local luminance pattern of two images to evaluate their resemblance or dissimilarity, and are positive constants. Once again, an image's brightness, contrast, and structure may be described in their own ways:

$$l(x,y) = \frac{2\mu_x\mu_y + C_1}{\mu_x^2 + \mu_y^2 + C_1}$$

$$c(x,y) = \frac{2\sigma_x\sigma_y + C_2}{\sigma_x^2 + \sigma_y^2 + C_2}$$

$$s(x,y) = \frac{\sigma_{xy} + C_3}{\sigma_x\sigma_y + C_3}$$

Where σ_x and σ_y the (local) sample standard deviations of x and y, respectively, μ_x and μ_y are the (local) sample means of x andy, respectively, and σ_{xy} is the (local) sample correlation coefficient between x and y. If $\alpha = \beta = \gamma = 1$, then the index is basic as the subsequent form utilizing Equations (1)-(3):

$$SSIM(x,y) = \frac{(2\mu_x\mu_y+C_1)(2\sigma_{xy}+C_2)}{(\mu_x^2+\mu_y^2+C_1)(\sigma_x^2\sigma_y^2+C_2)} \quad (5)$$

- **Region of Interest (ROI)**

The term "region of interest" (ROI) refers to a specific section of an image that has been singled out for closer inspection. We can determine the peak height, breadth, and average value from an area of interest (ROI), as well as the area under a curve. For instance, a count rate (number per time unit) registered spectrally, in time, or along a trajectory is one kind of measurement curve that may be recorded with the area of interest.

- **Canny edge detector**

Canny filters may identify edges in several stages. It employs a filter based on the derivative of a Gaussian in order to calculate the strength of the gradients. If there is noise in the picture, the Gaussian smoother will help smooth it out. The next step is to get rid of the pixels that are less than the maximum of the gradient magnitude, which would make the potential edges into 1-pixel curves. Last but not least, hysteresis thresholding is used to the gradient magnitude to conclude whether or not edge pixels are maintained. With the Canny, we may alter the low and high hysteresis thresholds as well as the width of the Gaussian (the wider the Gaussian, the messier the image).

The general criteria for edge detection include:

1. Accurately identifying the majority of visible edges in the image while maintaining a low error rate during detection.
2. An operator-detected edge point must precisely locate the geometrical center of the edge in order to be useful.
3. There should be no double-marking of edges in an image, and image noise shouldn't generate erroneous ones.

7. Results and Discussion

Image resizing: Adjust the image's size up or down (number of pixels). The number of pixels in both the horizontal and vertical dimensions is reduced by a factor of 2 When an

image is down sampled (resampled at a lower rate). When an image is upsampled (resampled at a greater rate), the pixel dimensions increase from 512 on a side to 1024 on the other. The raw MIAS data picture that was used in the analysis's preliminary processing. Images undergo preprocessing procedures include scaling, noise reduction, filtering, and brightness improvement. Results of picture preprocessing are shown in Figures 3 through 6, which span a range of frame sizes. Figures 7 and 8 show the ROI and edge detection images, respectively. Based on these established standards, the experimental outcomes of the proposed filtering approach on noised pictures are evaluated. The number of images and filters used in the studies were both set to their default values. How well the denoised image turns out depends heavily on how well the image numbers are initialized. Hence, a series of tests are carried out to determine the optimal value of the number of photographs.

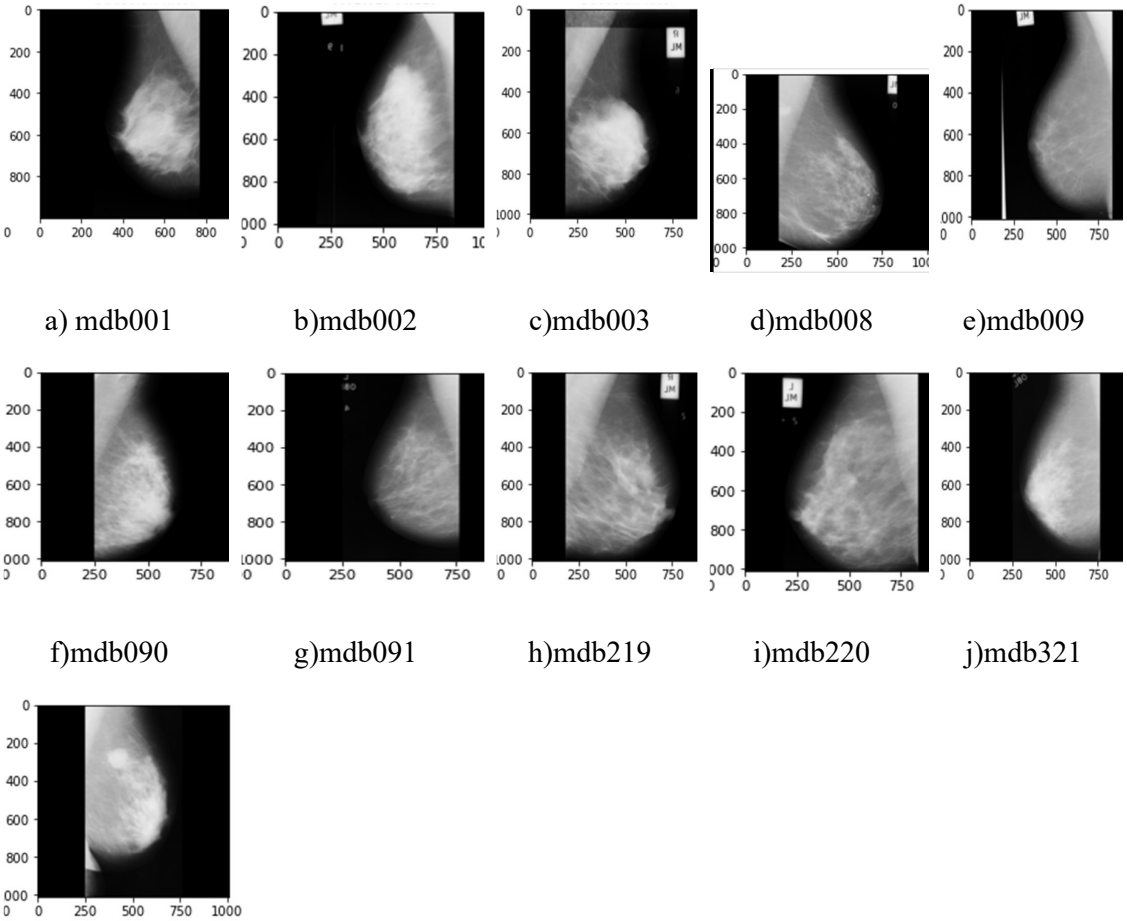

a) mdb001 b)mdb002 c)mdb003 d)mdb008 e)mdb009

f)mdb090 g)mdb091 h)mdb219 i)mdb220 j)mdb321

k)mdb322

Figure3. A Visualization Example of Denoised using the Wiener Filter

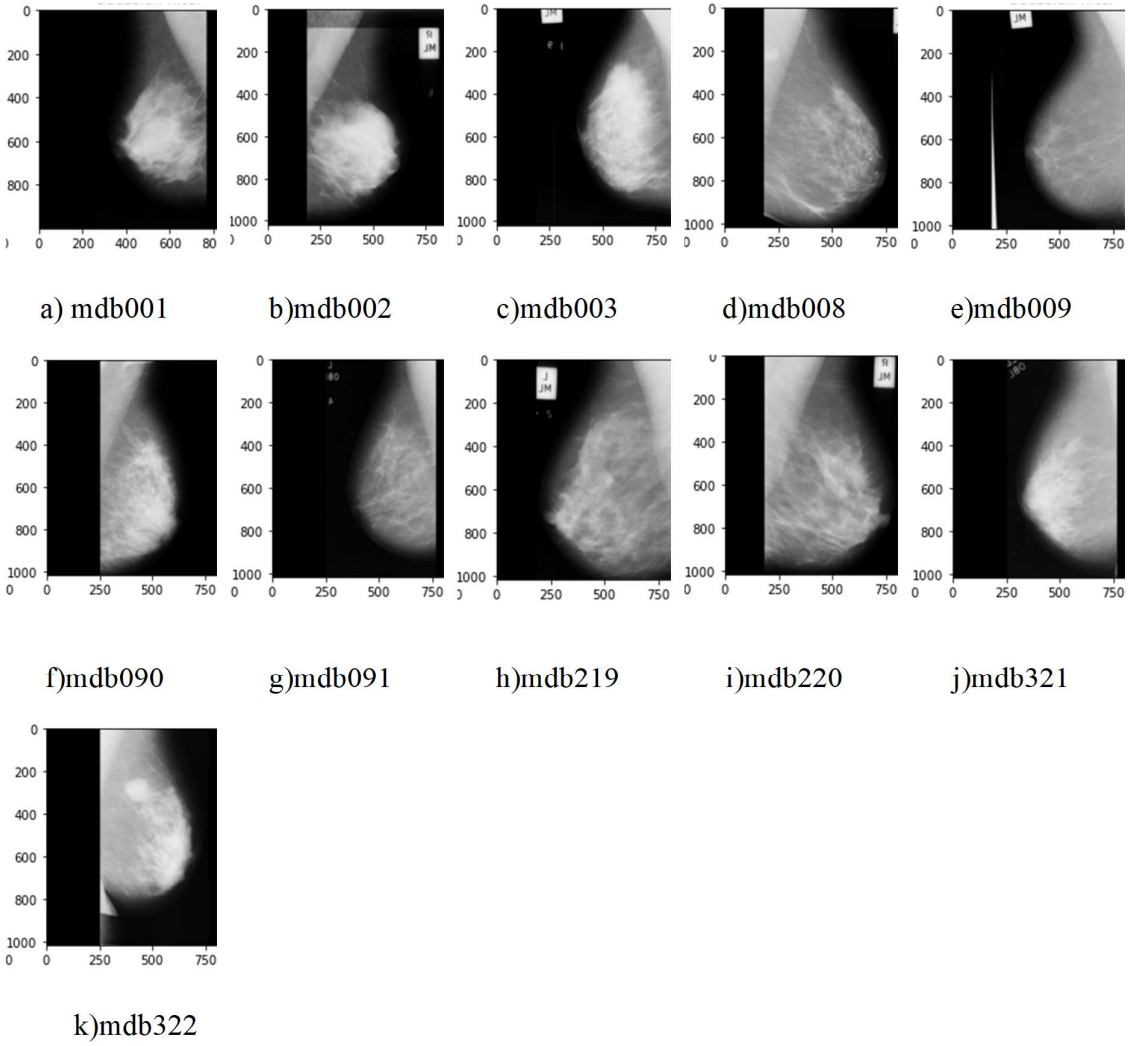

a) mdb001 b)mdb002 c)mdb003 d)mdb008 e)mdb009

f)mdb090 g)mdb091 h)mdb219 i)mdb220 j)mdb321

k)mdb322

Figure4. A Visualization Example of Denoised using the Gaussian Filter.

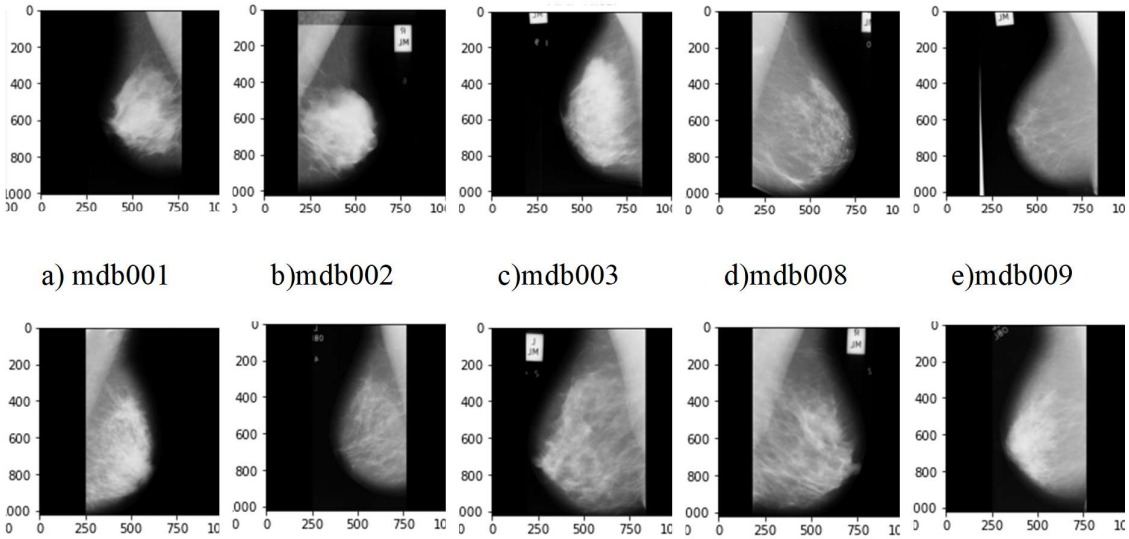

a) mdb001 b)mdb002 c)mdb003 d)mdb008 e)mdb009

f)mdb090 g)mdb091 h)mdb219 i)mdb220 j)mdb321

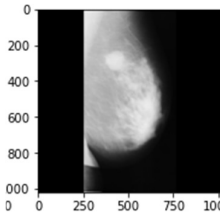

k)mdb322

Figure5. A Visualization Example of Denoised using the AMF Filter

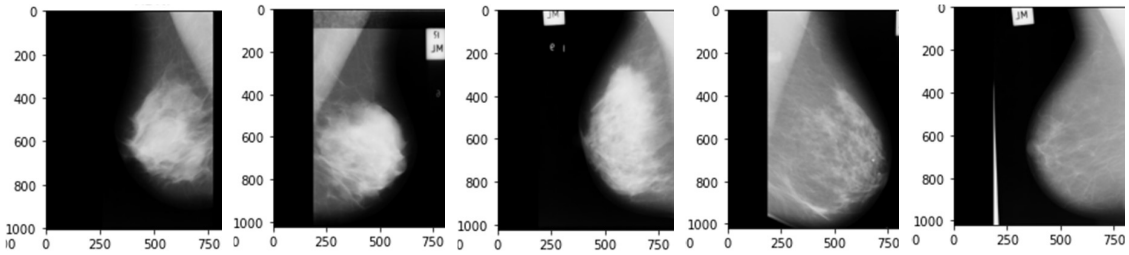

a) mdb001 b)mdb002 c)mdb003 d)mdb008 e)mdb009

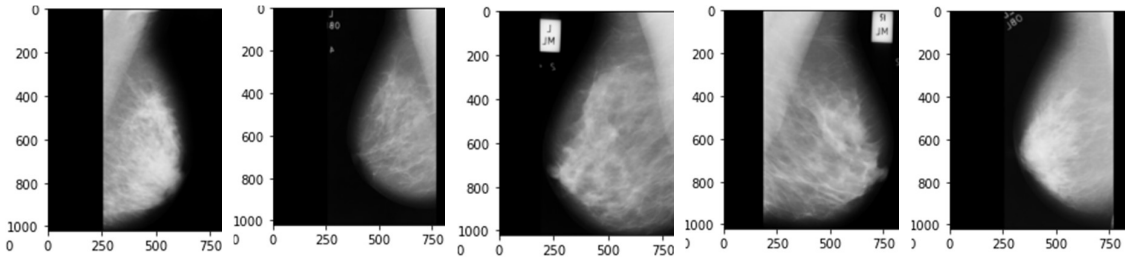

f)mdb090 g)mdb091 h)mdb219 i)mdb220 j)mdb321

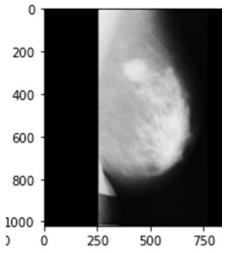

k)mdb322

Figure6. A Visualization Example of Denoised using the HDNF Filter

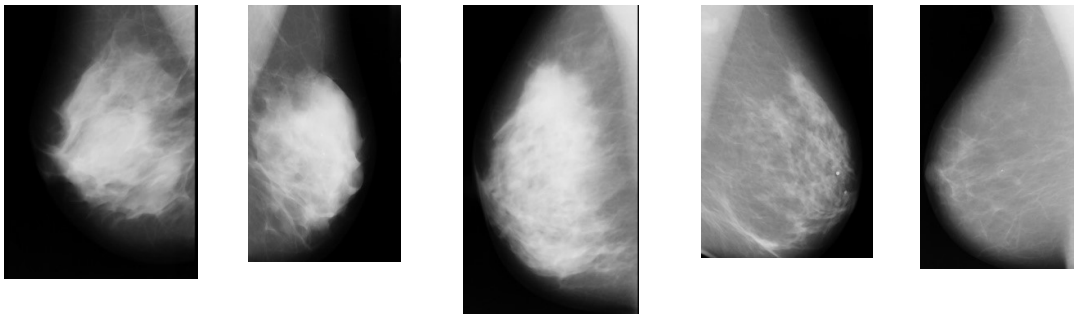

a)mdb001 b)mdb002 c)mdb003 d)mdb008 e)mdb009

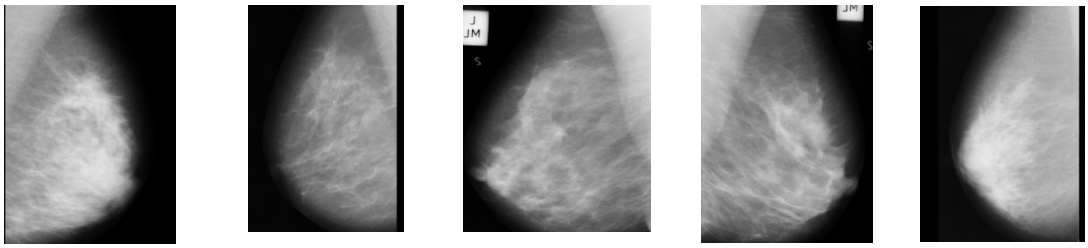

f)mdb090 g)mdb091 h)mdb219 i)mdb220 j)mdb321

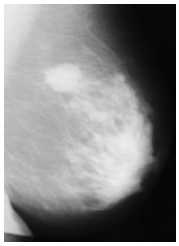

k)mdb322

Figure7. ROI image Process for Denosing breast cancer image,

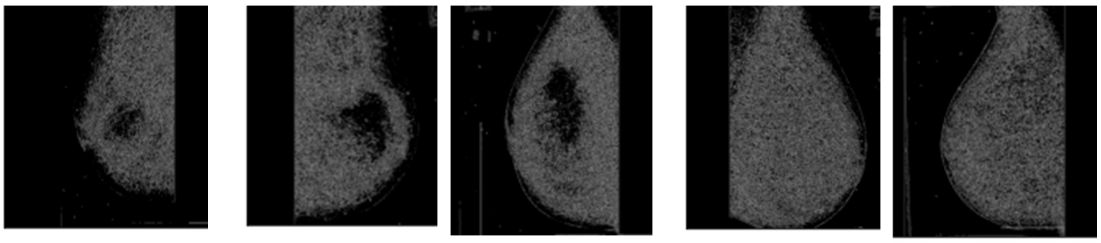

a)mdb001 b)mdb002 c)mdb003 d)mdb008 e)mdb009

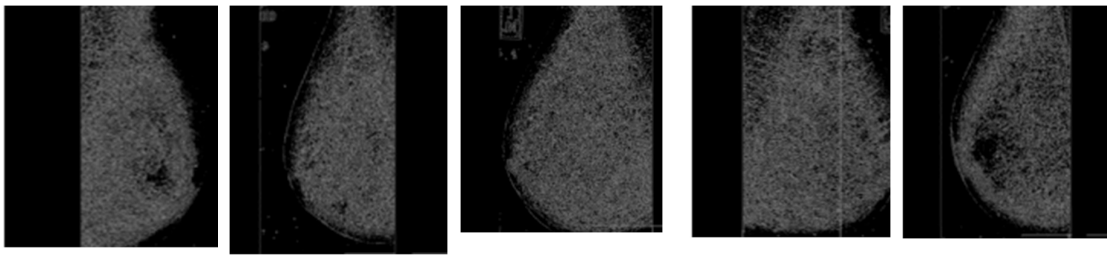

f)mdb090 g)mdb091 h)mdb219 i)mdb220 j)mdb321

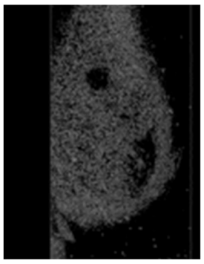

k)mdb322

Figure8. ROI image Process for Canny edge detection breast cancer image.

Quantitative findings for MSE, PSNR, and SSIM for three distinct breast cancer images are shown in Tables I, II, and III, respectively.

Table 1. Comparison Results of MSE Measure for Wiener Filter, Gaussian Filter, AMF And HDNF Methods

Image Name	Wiener Filter	Gaussian Filter	AMF	HDNF
mdb001.jpg	1.2908	0.42915	1.2918	0.0511
mdb002.jpg	2.7634	0.96126	2.7671	0.0814
mdn003.jpg	3.1118	1.09758	3.11557	0.1042
mdb008.jpg	2.7187	0.96700	5.8072	0.0831
mdb009.jpg	5.792	2.13475	2.7237	0.1284
mdb090.jpg	0.8999	0.4179	0.8991	0.0283
mdb091.jpg	1.7060	0.4964	1.7086	0.0514
mdb219.jpg	3.6985	1.1550	3.7055	0.0803
mdb220.jpg	2.6801	1.01028	2.6841	0.0931

mdb321.jpg	2.000	0.5527	2.0062	0.0509
mdb322.jpg	1.3316	0.6071	1.3329	0.3099

A measure of filter quality, MSE shows how well the filtered result matches the original. The fitness of the input and filtered output pictures will be closer together as the MSE value decreases. Based on the results of the experiments, HDNF is superior to other filters in its ability to remove noise since it has the lowest MSE values.

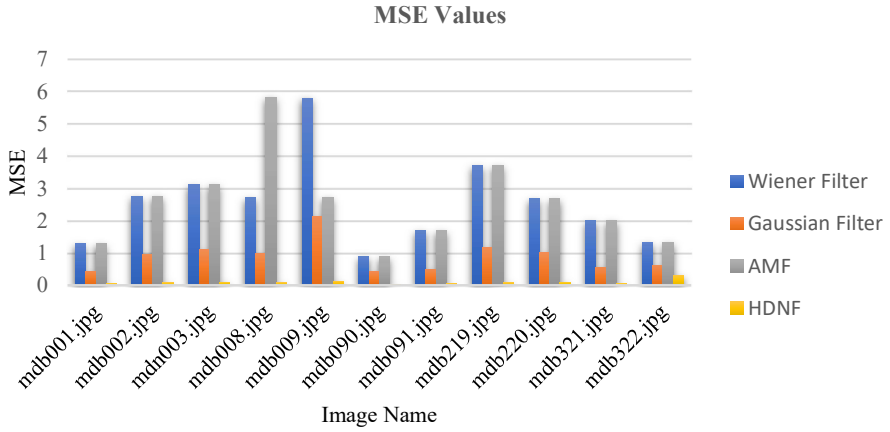

Figure9. Graphical represent of MSE values.

The PSNR measures the quality of a signal's representation according to the ratio of its greatest potential value to the value of corrupting noise. It is shown that the best filter is the one with the highest PSNR value. An examination of the filters' performances reveals that HDNF has the best PSNR of the four.

Table 2. Comparison Results of PSNR Measure for Wiener Filter, Gaussian Filter, AMF and HDNF Methods

Image Name	Wiener Filter	Gaussian Filter	AMF	HDNF
mdb001.jpg	41.1965	44.9111	41.2185	50.9219
mdb002.jpg	38.7054	41.023	38.7090	49.2931
mdn003.jpg	39.8402	42.829	39.8641	49.8051
mdb008.jpg	38.3454	41.4589	39.6890	49.1880
mdb009.jpg	39.6280	42.339	38.3601	48.5453
mdb090.jpg	40.37031	43.9545	40.3687	51.98392
mdb091.jpg	41.0374	44.4622	41.035	50.30185

mdb219.jpg	38.0966	41.6296	38.098	49.5849
mdb220.jpg	38.3197	41.6519	38.3278	48.8794
mdb321.jpg	41.1337	44.1675	41.1355	50.2805
mdb322.jpg	40.9792	44.5848	40.9751	51.6049

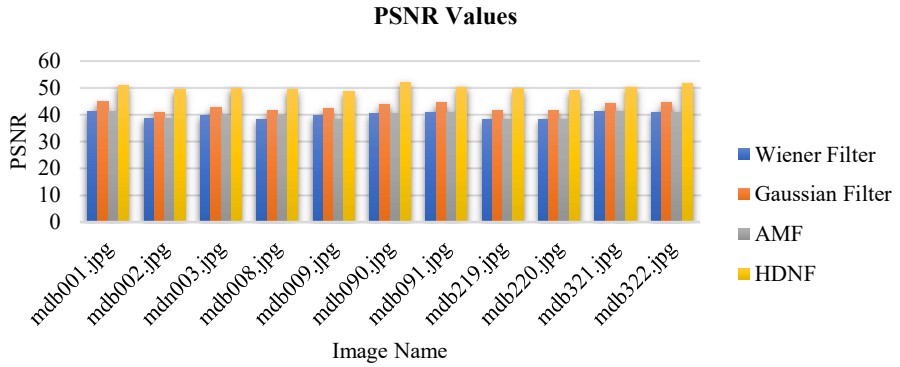

Figure10. Graphical represent of MSE values.

One way to evaluate how similar two photos are is with the use of the Structural Similarity Index (SSIM). The resultant SSIM index is a decimal number between -1 and 1, with 1 denoting complete structural similarity, which is only possible for two identical data sets. A score of 0 indicates there is no structural resemblance between the two entities. From among four filters, HDNF has the highest SSIM value.

Table 3. Comparison results of SSIM Measure for Wiener Filter, Gaussian Filter, AMF And HDNF Methods

Image Name	Wiener Filter	Gaussian Filter	AMF	HDNF
mdb001.jpg	0.9641	0.9797	0.9654	0.9986
mdb002.jpg	0.93786	0.9609	0.93873	0.9983
mdn003.jpg	0.9468	0.9673	0.94869	0.9983
mdb008.jpg	0.9345	0.9649	0.94169	0.9979
mdb009.jpg	0.9374	0.9619	0.9364	0.9979
mdb090.jpg	0.9638	0.9789	0.9643	0.9988
mdb091.jpg	0.9606	0.9787	0.9609	0.9985
mdb219.jpg	0.9320	0.9647	0.9325	0.9980

mdb220.jpg	0.9376	0.9657	0.9384	0.99803
mdb321.jpg	0.9617	0.9788	0.9617	0.9984
mdb322.jpg	0.9704	0.9826	0.9705	0.9986

Figure11. Graphical represent of MSE values.

8. Conclusion

The defects and noises that occur during the capture of mammography images have an impact on image processing and ROI diagnosis in breast cancer. The Canny Edge Detector method performs best. Noise reduction during preparation is a more difficult task. For the purpose of denoising mammography breast cancer pictures, this work used four distinct filtering algorithms (the Wiener Filter, GF, AMF, and HDNF). We analyze the filters' performance and make comparisons based on the quality metrics of PSNR, MSE, and SSIM. Experiments on mammography breast cancer pictures show that HDNF is effective in removing noise.

References

[1] Saffari, Nasibeh, Hatem A. Rashwan, Mohamed Abdel-Nasser, Vivek Kumar Singh, Meritxell Arenas, Eleni Mangina, Blas Herrera, and Domenec Puig. "Fully Automated Breast Density Segmentation and Classification Using Deep Learning." Diagnostics 10, no. 11 (2020): 988.

[2] Li, Jianqiang, Yan Pei, Anaa Yasin, Saqib Ali, and Tariq Mahmood. "Computer Vision-Based Microcalcification Detection in Digital Mammograms Using Fully Connected Depthwise Separable Convolutional Neural Network." Sensors 21, no. 14 (2021): 4854.

[3] Rouhi, Rahimeh, Mehdi Jafari, Shohreh Kasaei, and Peiman Keshavarzian. "Benign and malignant breast tumors classification based on region growing and CNN segmentation." Expert Systems with Applications 42, no. 3 (2015): 990-1002.

[4] Vikramathithan, A. C., Sourabh V. Bhat, and D. R. Shashikumar. "Denoising High-Density Impulse Noise using Duo-Median Filter for Mammogram Images." In 2020 International Conference on Smart Technologies in Computing, Electrical and Electronics (ICSTCEE), pp. 610-613. IEEE, 2020.

[5] Boby, Shakil Mahmud, and Shaela Sharmin. "Medical Image Denoising Techniques against Hazardous Noises: An IQA Metrics Based Comparative Analysis." (2021).

[6] Suneetha, Mopidevi, and Mopidevi Subbarao. "An Improved Denoising of Medical Images Based on Hybrid Filter Approach and Assess Quality Metrics." In Journal of Biomimetics, Biomaterials and Biomedical Engineering, vol. 44, pp. 27-36. Trans Tech Publications Ltd, 2020.

[7] Tang, Siyi, Amirata Ghorbani, Rikiya Yamashita, Sameer Rehman, Jared A. Dunnmon, James Zou, and Daniel L. Rubin. "Data valuation for medical imaging using Shapley value and application to a large-scale chest X-ray dataset." Scientific reports 11, no. 1 (2021): 1-9.

[8] Pallavi Bora, Kapil Chaudhary. “Improved Image Denoising Methodology using Deep CNN Bilateral Filter Compared to Additional Methods.” International Journal of Engineering and Advanced Technology (IJEAT) ISSN: 2249-8958 (Online), Volume-10 Issue-5, June 2021.

[9] MehmoodGondal, Rashid, Saima Anwar Lashari, Murtaja Ali Saare, and Sari Ali Sari. "A hybrid de-noising method for mammogram images." Indonesian Journal of Electrical Engineering and Computer Science 21, no. 3 (2021): 1435-1443.

[10] R. Sammouda, A. M. S. Al-Salman, A. Gumaei, and N. Tagoug, "An efficient image denoising method for wireless multimedia sensor networks based on DT-CWT," International Journal of Distributed Sensor Networks, vol. 11, no. 11, p. 632568, 2015.

[11] Venkataramanan, Abhinau K., Chengyang Wu, Alan C. Bovik, Ioannis Katsavounidis, and Zafar Shahid. "A Hitchhiker’s Guide to Structural Similarity." IEEE Access 9 (2021): 28872-28896.

[12] Ahuja, Avani, Lidia Al-Zogbi, and Axel Krieger. "Application of Noise-Reduction Techniques to Machine Learning Algorithms for Breast Cancer Tumor Identification." Computers in Biology and Medicine (2021): 104576.

[13] Mendes, João, and Nuno Matela. "Breast Cancer Risk Assessment: A Review on Mammography-Based Approaches." Journal of Imaging 7, no. 6 (2021): 98.

[14] Khamparia, Aditya, Subrato Bharati, Prajoy Podder, Deepak Gupta, Ashish Khanna, Thai Kim Phung, and Dang NH Thanh. "Diagnosis of breast cancer based on modern mammography using hybrid transfer learning." Multidimensional systems and signal processing 32, no. 2 (2021): 747-765.

[15] Yu, Xiangchun, Wei Pang, Qing Xu, and Miaomiao Liang. "Mammographic image classification with deep fusion learning." Scientific Reports 10, no. 1 (2020): 1-11.

[16] Yan, Rui, Fa Zhang, Xiaosong Rao, Zhilong Lv, Jintao Li, Lingling Zhang, Shuang Liang, et al. "Richer fusion network for breast cancer classification based on multimodal data." BMC Medical Informatics and Decision Making 21, no. 1 (2021): 1-15.